

# Fabrication and characterization of polymer-derived $\text{Si}_2\text{N}_2\text{O}-\text{ZrO}_2$ nanocomposite ceramics

V. M. SGLAVO, R. DAL MASCHIO, G. D. SORARÙ

*Dipartimento di Ingegneria dei Materiali, Università dei Trento, via Mesiano 77, I-38050 Trento, Italy*

A. BELLOSI

*CNR Istituto di Ricerche Tecnologiche per la Ceramica, via Granarolo 64, I-48018 Faenza, Italy*

Amorphous Si–Zr–N–O powders, obtained by nitridation in an  $\text{NH}_3$  flow of zirconium modified polycarbosilane, have been sintered to full density by hot pressing at  $1500^\circ\text{C}$ . The resulting ceramic shows an extremely fine-grained microstructure composed of  $\text{Si}_2\text{N}_2\text{O}$  and  $\text{ZrO}_2$  crystallites 20–30 nm in diameter. Thermal stability measured in air appears excellent up to  $1300^\circ\text{C}$  for 48 h. Mechanical characterization pointed out good values of flexural strength (330 MPa), fracture toughness ( $4.1 \text{ MPa m}^{0.5}$ ) and Weibull modulus.

## 1. Introduction

Highly covalent ceramics such as SiC and  $\text{Si}_3\text{N}_4$  can now be prepared by pyrolysis of metal–organic polymers. This new method has been first applied to the fabrication of silicon carbide fibres from polycarbosilane [1]. Since then it has been exploited mainly in the preparation of fibres of many different ceramic systems [2]. More recently, the polymer route has been considered as a unique method to obtain amorphous ceramic phases [3]. Indeed, the as-pyrolysed material usually displays a disordered microstructure that transforms into a microcrystalline ceramic upon increasing the pyrolysis temperature [4]. Few studies have been devoted to the use of these amorphous materials as starting powders in the traditional sintering of ceramics [5–7]. In fact, a higher sinterability with the formation of a fine-grained microstructure at lower temperatures can be expected compared to that of crystalline powders.

Recently, some of the present authors, have shown that alkoxide-modified polycarbosilanes are suitable precursors for silicon carbide and silicon nitride-based ceramics [8, 9]. According to these results, an amorphous Si–N–Zr–O phase is obtained from the pyrolysis, in flowing ammonia, of a polyzirconocarbosilane (PZC) synthesized reacting zirconium *n*-propoxide and polycarbosilane [10]. By increasing the temperature up to  $1500^\circ\text{C}$  this disordered solid leads to the formation of very fine tetragonal zirconia crystals embedded into a silicon nitride matrix [10].

Silicon nitride and silicon oxynitride have been identified as promising structural ceramics due to the combination of various properties, such as excellent strength and creep resistance over a wide range of temperature, good corrosion resistance, low specific weight and high electrical resistivity. Moreover, the

addition of  $\text{ZrO}_2$  increase the strength and fracture toughness of both  $\text{Si}_3\text{N}_4$  [11, 12] and  $\text{Si}_2\text{N}_2\text{O}$  [13]. However, the sintering process of silicon oxynitride and silicon nitride materials requires a high sintering temperature and high nitrogen pressures to hinder decomposition reactions. To overcome these problems, oxide additives giving a liquid phase are generally used to allow the formation of fully dense ceramics at lower temperatures via a liquid-phase sintering process. Indeed, dense  $\text{Si}_2\text{N}_2\text{O}$  has recently been produced either by pressureless sintering [14, 15] using large amounts of sintering aids (10 wt %  $\text{Y}_2\text{O}_3$  and 6%  $\text{Al}_2\text{O}_3$ ) or by glass-encapsulation hot isostatic pressing (HIP) at  $1950^\circ\text{C}$  [16].

As with the addition of  $\text{ZrO}_2$ , the main problem associated with the fabrication of  $\text{Si}_3\text{N}_4$  and/or  $\text{Si}_2\text{N}_2\text{O}-\text{ZrO}_2$  composites, is the formation of zirconium oxynitrides. Reaction between  $\text{Si}_3\text{N}_4$  and  $\text{ZrO}_2$  may occur at high temperatures producing undesirable phases such as zirconium oxynitride and ZrN [17]. Zirconium oxynitride readily reacts with oxygen at low temperature ( $\approx 500^\circ\text{C}$ ) to produce monoclinic zirconia and gaseous nitrogen with a molar volume increase of  $\approx 5\%$  causing a severe degradation of the material [12]. The formation of these nitrogen-containing phases during densification can be suppressed by using  $\text{Y}_2\text{O}_3$ -stabilized  $\text{ZrO}_2$  as starting powder [12] or by decreasing the sintering temperatures [18, 19].

In this study, in order to decrease the processing temperature of dense  $\text{Si}_2\text{N}_2\text{O}-\text{ZrO}_2$  composite ceramics and with the aim of obtaining a homogeneous fine-grained microstructure, the use of highly-reactive, polymer-derived amorphous Si–N–Zr–O powders has been attempted. This paper describes the fabrication of this material as well as its microstructural and

mechanical characterization. Results are discussed and compared with literature data on similar materials.

## 2. Experimental procedure

Polyzirconocarbosilane was prepared by reacting polycarbosilane (Dow Corning) and zirconium *n*-propoxide (Fluka) following a procedure described in detail elsewhere [10]. PZC polymer was pyrolysed at  $5^\circ\text{C min}^{-1}$  in a silica tube in flowing  $\text{NH}_3$  at  $1000^\circ\text{C}$  for 1 h to obtain the amorphous Si–Zr–N–O phase. The as-produced white powders were mixed with  $\text{Al}_2\text{O}_3$  (5 wt %) as a sintering aid and attritor milled in a plastic jar for 20 min in isobutyl alcohol. Disc specimens (40 mm diameter  $\times$  7 mm width) were fabricated by hot-pressing 30 g powder at  $1500^\circ\text{C}$  and 30 MPa for 20 min under vacuum in an induction-heated graphite die. Continuous shrinkage of the sample was recorded during hot pressing.

Density measurements were performed by the Archimedes' method using distilled water as fluid. Phase analysis was performed by collecting X-ray diffraction (XRD) spectra on a spectrometer operating at 20 kV with a  $\text{CuK}_\alpha$  radiation and a nickel filter. Crystal size was estimated from the width of the XRD peaks using the Scherrer equation.

Specimens for oxidation tests were cut from hot-pressed discs into square bars (2 mm  $\times$  2 mm  $\times$  12 mm); the oxidation resistance was measured by heating samples in air and continuously recording the weight changes by thermogravimetry. Specimens were heat-treated in air at temperatures of 900 and  $1300^\circ\text{C}$  and holding times of 48 h were used.

The coefficient of thermal expansion was determined over the temperature range  $20$ – $1300^\circ\text{C}$  in air at a heating rate  $5^\circ\text{C min}^{-1}$ , on 3 mm  $\times$  3 mm  $\times$  15 mm samples.

Hot-pressed specimens were machined for the preparation of bend-test bars (25 mm  $\times$  3 mm  $\times$  3 mm). One of the surfaces of the test bars was ground and polished with diamond pastes up to 1  $\mu\text{m}$ . Bend tests were carried out using a universal mechanical testing machine by three-point bending with a span of 20 mm. Testing was conducted on 14 samples at room temperature with a crosshead speed of  $1\text{ mm min}^{-1}$ . Fracture surfaces analysis was performed by scanning electron

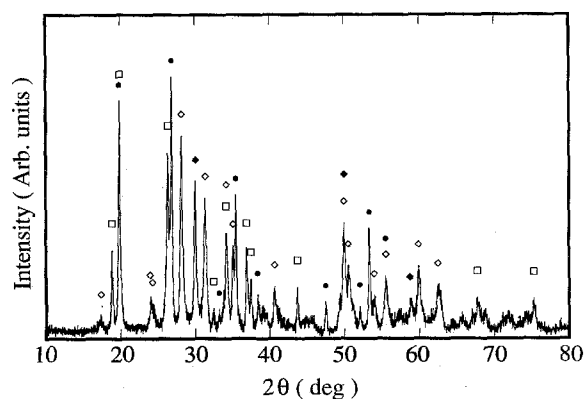


Figure 1 X-ray diffractogram of the hot-pressed ceramic. (□)  $\text{Si}_2\text{N}_2\text{O}$ , (◇) *m*- $\text{ZrO}_2$ , (◈) *t*- $\text{ZrO}_2$ , (●)  $\text{ZrSiO}_4$ .

microscopy in order to obtain information concerning the nature and location of the strength-controlling flaws.

Elastic modulus was evaluated by the resonance frequency method. Vickers hardness, *H*, and critical stress intensity factor,  $K_{\text{IC}}$ , were evaluated by indentation techniques on polished surfaces. Hardness was obtained using loads ranging from 5–100 N. The fracture toughness expression proposed by Niihara *et al.* [20] for indentation-generating median cracks was adopted to estimate the  $K_{\text{IC}}$  value, using loads of 70 and 100 N.

## 3. Results and discussion

### 3.1. Densification and microstructure

A density of  $3.38\text{ g cm}^{-3}$  was measured on the sintered sample. Chemical analysis performed on the starting polymer and on the HP ceramic gave Zr/Si = 0.14. The XRD spectrum, shown in Fig. 1, reveals the presence of  $\text{Si}_2\text{N}_2\text{O}$  and  $\text{ZrO}_2$ ; the latter both in the tetragonal and monoclinic form. A  $\text{SiZrO}_4$  phase was also detected. No evidence of the formation of zirconium oxynitride phases has been found from the XRD analysis.

The structural evolution up to  $1500^\circ\text{C}$  of the amorphous Si–Zr–N–O powders produced from nitridation of PZC have been already extensively characterized by means of XRD analysis and magic angle spinning–nuclear magnetic resonance (MAS–NMR) spectroscopy [10]. For samples heated at  $1500^\circ\text{C}$ , the diffraction spectra revealed mainly the presence of crystalline  $\beta$ - $\text{Si}_3\text{N}_4$  and tetragonal  $\text{ZrO}_2$ . Moreover,  $^{29}\text{Si}$  MAS–NMR experiments suggested the existence of a glassy silicon-oxynitride phase. The formation of this glassy phase is due to the excess of oxygen introduced in the polymer precursor via the zirconium alkoxide ( $\text{O/Zr} = 4$ ) and to the high reactivity of the amorphous Si–Zr–N–O powders towards ambient moisture which leads to an increase of the overall oxygen content. In the present case the complete absence, in the sintered sample, of  $\text{Si}_3\text{N}_4$  and the formation of  $\text{Si}_2\text{N}_2\text{O}$  and  $\text{SiZrO}_4$ , can be accounted for by an extensive oxygen pick-up during the milling process. In fact, similar results concerning the formation of pure  $\text{Si}_2\text{N}_2\text{O}$  ceramics from polysilazane-derived amorphous silicon nitride powders have recently been reported in the literature [7].

From the measured value of Si/Zr, theoretical density can be estimated by considering the density of the pure phases ( $\rho_{\text{Si}_2\text{N}_2\text{O}} = 2.82$ ,  $\rho_{\text{ZrO}_2} = 5.90$ ,  $\rho_{\text{SiZrO}_4} = 4.67\text{ g cm}^{-3}$ ) and assuming that all zirconium atoms, in a first case form  $\text{ZrO}_2$  and in a second one,  $\text{SiZrO}_4$ . The calculated density values range from  $3.26$ – $3.31\text{ g cm}^{-3}$  respectively. These values agree well with the experimental one and suggest the formation of a fully dense material. SEM analysis, discussed later, substantiates the pore-free nature of the hot-pressed ceramic.

The densification behaviour during hot pressing of the Si–Zr–N–O amorphous powders with the addition of 5 wt %  $\text{Al}_2\text{O}_3$  is shown in Fig. 2. Relative density is plotted against temperature up to  $1500^\circ\text{C}$

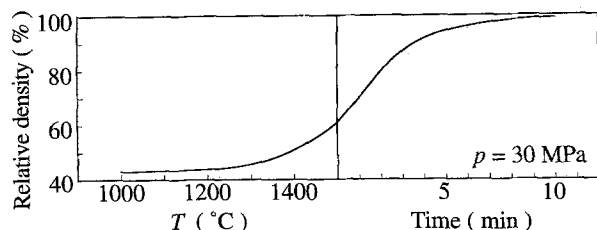


Figure 2 Densification curve during hot pressing as a function of temperature and for the isothermal at 1500 °C.

and then against time during the isothermal run at 1500 °C.

The shrinkage starts at about 1000 °C from a green density of  $\approx 43\%$ . The densification rate increases very slowly up to about 1300 °C, then increases rapidly and reaches a maximum at 1500 °C in correspondence with the relative densities in the range 65%–75%. From the observed behaviour it may be shown that densification proceeds via a liquid-phase sintering mechanism, as proposed by Kingery *et al.* [21], and which has been previously observed for almost all the silicon nitride or silicon oxynitride based materials [22–25].

Three stages of densification are recognized in the Kingery model: initially the particle fragmentation and rearrangement stage can be evaluated as a flux of matter through the contact regions to the surface of the neck between solid particles. When a liquid phase forms, it wets and penetrates among the particles and consequently a fast rearrangement of solid takes place by sliding over one another with little friction among them. In the second stage, material is dissolved from the necks into the liquid, transported away from the neck and reprecipitated elsewhere in areas of lower stress. The equation governing this important second stage is

$$\Delta L/L_0 = Kt^{1/n} \quad (1)$$

where  $\Delta L/L_0$  is the shrinkage at time  $t$ ,  $K$  is a constant and  $n$  assumes values which depend on the densification mechanism and on the shape of starting solid particles.

The third stage of densification is elimination of closed porosity but it is small in extent and does not significantly increase the final bulk density.

The applicability of the liquid-phase sintering model may be assumed on the basis of Fig. 3, only with reference to the second stage, as the first stage occurs during heating up to 1500 °C. In the second stage, under isothermal conditions, as the starting Si–Zr–N–O amorphous particles can be assumed to be spheroidal,  $n$  has a value of 2 if solution is the rate-controlling step, and 3 if diffusion through the liquid is rate-controlling. Therefore, as  $n = 3$ , diffusion of material from the interparticle neck through the liquid can be proposed as the mechanism governing the densification, in agreement with the results previously observed for the densification of various silicon nitride-based materials such as  $\beta'$ -SiAlON and O'-SiAlON [24].

The liquid formation and its characteristics (composition and viscosity) are strongly influenced by

$\text{Al}_2\text{O}_3$  which decreases the melting temperature by forming an aluminium silicate melt. The liquid enhances the dissolution of the starting solid particles and in this way, during the second stage, silicon, aluminium, oxygen and nitrogen are removed from the liquid and precipitate as  $\text{Si}_2\text{N}_2\text{O}$  and/or O'-SiAlON: this precipitation is rapid and completed with depletion of liquid after a short time. Actually, the presence of aluminium oxide plays a special role because the simultaneous equivalent substitution of Al–O for Si–N in  $\beta$ - $\text{Si}_3\text{N}_4$  and  $\text{Si}_2\text{N}_2\text{O}$  resulting in the formation of  $\beta'$ -SiAlON and O'-SiAlON, is well established [26, 27]. Therefore, it can be assumed that in our material,  $\text{Si}_2\text{N}_2\text{O}$  should contain in solid solution almost all the added alumina. At the same time also, part of the zirconia dissolves in the liquid and during cooling forms some zircon as second phase. The remaining part of the zirconia is present in the dense material in monoclinic or tetragonal form.

A study of the diffraction peaks according to the Scherrer equation resulted in an extraordinarily fine average crystal size of  $\approx 30$  nm for both  $\text{Si}_2\text{N}_2\text{O}$  and  $\text{SiZrO}_4$  and 20–25 nm for monoclinic and tetragonal zirconia. In fact, the stability at room temperature of non-stabilized tetragonal zirconia must be related to its very small crystal size, lower than 30 nm [28].

Scanning electron micrographs obtained on fracture surfaces agree with the density results showing a fully dense, pore-free microstructure. Observations at high magnification (Fig. 4) substantiate the nano-sized nature of the crystalline phases revealed by the XRD study.

### 3.2. Thermal properties

Experimental results, reported in Table I agree well with oxidation resistance properties by O'Meara *et al.* [29] for pressureless sintered  $\text{Si}_2\text{N}_2\text{O}$  materials confirming the excellent oxidation resistance of this type of ceramics. Moreover, this experimental evidence also agrees with the XRD results showing the complete absence, in the sintered ceramic, of the easily oxidizable zirconium-oxynitride phase.

The thermal expansion coefficient for the intervals 20–700 and 20–1300 °C was determined to be  $\alpha = 6.1 \times 10^{-6}$  and  $4.8 \times 10^{-6} \text{ } ^\circ\text{C}^{-1}$ , respectively.

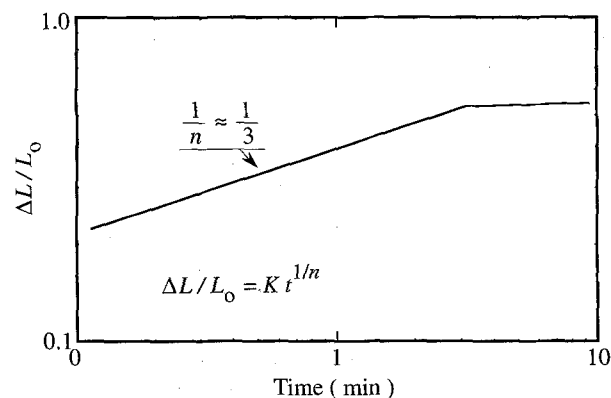


Figure 3 Shrinkage of the specimen during hot pressing under isothermal conditions 1500 °C.

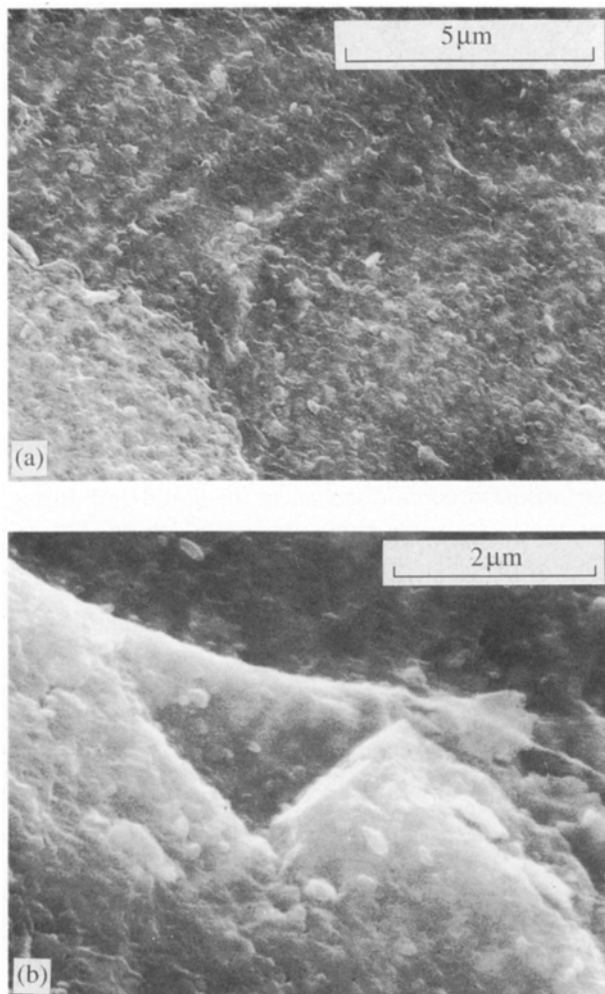


Figure 4 Scanning electron micrographs of the fracture surface of the hot-pressed ceramic.

TABLE I Weight gain of the hot-pressed ceramic after 48 h isotherm treatment in air

Temperature (°C)	Weight gain	
	per unit surface area (mg cm <sup>-2</sup> )	(%)
900	< 0.1	< 0.1
1300	1.47	0.44

TABLE II Vickers hardness at different loads for the hot-pressed ceramic

Load (N)	H (GPa)
5	14.7 ± 0.8
50	12.3 ± 0.1
100	12.0 ± 0.3

TABLE III Elastic modulus,  $E$ , fracture toughness,  $K_{IC}$ , modulus of rupture, MOR, and Weibull modulus,  $m$ , for the hot-pressed ceramic

$E$ (GPa)	$K_{IC}$ (MPa m <sup>0.5</sup> )	MOR (MPa)	$m$
191	4.1 ± 0.5	328 ± 35	10.9

### 3.3. Mechanical properties

Experimental results are reported in Tables II and III and will be discussed in comparison with data corresponding to related silicon oxynitride materials [7, 13, 16, 30–32].

Modulus of rupture shows a superior performance in comparison to that of fully dense monolithic Si<sub>2</sub>N<sub>2</sub>O (HIPed at 1570–1750 °C with a pressure of 33 MPa) studied by Billy *et al.* [30] and compared with polysilazane-derived Si<sub>2</sub>N<sub>2</sub>O by Seherer and Riedel [7]; on the other hand, it is comparable with MOR values presented by Larker [16] for Si<sub>2</sub>N<sub>2</sub>O HIPed at extremely high temperature and pressure. Comparison of fracture toughness with data presented in the previous papers seems to be hazardous, owing to the high variability depending on the measurement method. However,  $K_{IC}$  values in Table II indicate a reasonable agreement with data proposed by Billy *et al.* [30] and Rundgren *et al.* [13]. A clear improvement is evident in comparison to values of ≈ 3 MPa m<sup>0.5</sup> presented by Larker [16]. Both hardness and elastic modulus seems to be lower than those presented in other papers [16, 30–32]. Theoretical Young's modulus was estimated by the mixture rule following the same procedure proposed for densities calculations. The calculated elastic modulus values range from 254–275 GPa suggesting the presence of a glassy phase in the final well-densified material.

Scanning electron microscopy investigations of the fracture surfaces failed in revealing any typical defect such as pores, agglomerates or chemical inhomogeneity, suggesting that the hot-pressed ceramic has an highly homogeneous nano-sized microstructure in agreement with the high value of the Weibull modulus.

### 4. Conclusions

Highly reactive amorphous Si–Zr–N–O ceramic powders have been obtained from the nitridation process in an NH<sub>3</sub> flow of a polycarbosilane modified with a zirconium propoxide. These non-crystalline materials have been used to fabricate, at relatively low temperatures, a nano-composite ceramic of the system Si<sub>2</sub>N<sub>2</sub>O–ZrO<sub>2</sub>. XRD and SEM studies clearly indicated that the grain-size dimensions are in the range 20–30 nm. The hot-pressed material showed an excellent oxidation resistance in the temperature range 900–1300 °C. Moreover, the homogeneous and fine-grained microstructure resulted in promising values of mechanical properties such as MOR (330 MPa),  $K_{IC}$  (4.1 MPa m<sup>0.5</sup>) and Weibull modulus.

### Acknowledgements

The authors thank CNR for financial support. G. D. Sorarù also thanks Dr Florence Babonneau for helpful discussions.

### References

1. S. YAJIMA, M. OMORI, J. HAYASHI, K. OKAMURA, T. MATSUZAWA and C. F. LIAW, *Chem. Lett.* **551** (1976).
2. J. LIPOWITZ, *Am. Ceram. Soc. Bull.* **70** (1991) 1888.

3. G. D. SORARÛ, F. BABONNEAU and J. D. MACKENZIE, *J. Non-Cryst. Solids* **106** (1988) 256.
4. B. A. BENDER, R. W. RICE and J. R. SPANN, *J. Am. Ceram. Soc.* **70** (1989) C58.
5. H. KODAMA, T. MYOSHI, *Adv. Ceram. Mater.* **3** (1988) 177.
6. R. RIEDEL, M. SEHER and G. BECKER, *J. Eur. Ceram. Soc.* **5** (1989) 113.
7. M. SEHER and R. RIEDEL, "Proceedings of the 2nd European Ceramic Society Conference", 11–14 September 1991, Ausburg, Germany, in press.
8. G. D. SORARÛ, F. BABONNEAU and J. D. MACKENZIE, in "Better Ceramics Through Chemistry IV", edited by B. J. J. Zelinski, C. J. Brinker, D. E. Clark and D. R. Ulrich, Pittsburgh, PA, Materials Research Society Symposium Proceedings, Vol. 180 (MRS, San Francisco, 1990), p. 815.
9. G. D. SORARÛ, A. RAVAGNI, R. DAL MASCHIO and F. BABONNEAU, in "Proceedings of the 2nd European Ceramic Society Conference", 11–14 September 1991, Ausburg, Germany, in press.
10. G. D. SORARÛ, A. RAVAGNI, R. DAL MASCHIO, G. CARTURAN and F. BABONNEAU, *J. Mater. Res.* **7** (1992) 1266.
11. N. CLAUSSEN and J. JAHN, *J. Am. Ceram. Soc.* **61** (1978) C94.
12. F. F. LANGE, *ibid.* **63** (1980) 38.
13. K. RUNDGREN, J. BRANDT and R. POMPE, in "Proceedings of the 2nd European Ceramic Society Conference", 11–14 September 1991, Ausburg, Germany, in press.
14. M. H. LEWIS, C. J. REED and N. D. BUTLER, *Mater. Sci. Eng.* **71** (1985) 87.
15. C. O'MEARA and J. SJOBERG, in "Ceramic Transactions", Vol. 7 (American Ceramic Society, 1990) p. 647.
16. R. LARKER, *J. Am. Ceram. Soc.* **75** (1992) 62.
17. T. EKSTROM, L. K. L. FALK and E. M. KNUDSON-WEDEL, *J. Mater. Sci.* **26** (1991) 4331.
18. J. WEISS, J. GAUCKLER and T. Y. TIEN, *J. Amer. Ceram. Soc.* **63** (1979) 632.
19. A. K. TJERNLUND, R. POMPE, M. HOLMSTROM and R. CARLSSON, *Brit. Ceram. Proc.* **37** (1986) 29.
20. K. NIIHARA, R. MORENA and D. P. H. HASSELMAN, *J. Mater. Sci. Lett.* **1** (1982) 13.
21. W. D. KINGERY, J. M. VOLBROUND and F. R. CHARVAT, *J. Am. Ceram. Soc.* **46** (1963) 391.
22. A. BELLOSI, P. VINCENZINI and G. N. BABINI, *Mater. Chem. Phys.* **18** (1987) 205.
23. S. A. SIDDIQI, I. HIGGING and A. HENDRY, in "Non-oxide Technical and Engineering Ceramics", edited by S. Hampshire (Elsevier Applied Science, London, 1986) p. 1.
24. M. B. TRIGG and K. H. JACK, *J. Mater. Sci.* **23** (1988) 481.
25. Z. K. HUANG, P. GREIL and G. PETZOW, *Ceram. Int.* **10**(1) (1984) 14.
26. K. H. JACK, in "Non-oxide Technical and Engineering Ceramics", edited by S. Hampshire (Elsevier Applied Science, London, 1986) p. 1.
27. M. B. TRIGG and K. H. JACK, *J. Mater. Sci. Lett.* **6** (1987) 407.
28. A. H. HEUER, N. CLAUSSEN, W. M. KRIVEN and M. RÜHLE, *J. Am. Ceram. Soc.* **65** (1982) 642.
29. C. O'MEARA, J. SIOBERG, G. DUNLOP and R. POMPE, *J. Eur. Ceram. Soc.* **7** (1991) 369.
30. M. BILLY, P. BOCH, C. DUMAZEAU, J. C. GLANDUS and P. GOURSAT, *Ceram. Int.* **7** (1981) 13.
31. J. C. GLANDUS and P. BOCH, in "Nitrogen Ceramics", edited by F. L. Riley (Nordhoff, Leyden, 1977) p. 515.
32. P. BOCH and J. C. GLANDUS, in "Progress in Nitrogen Ceramics", edited by F. L. Riley (Martinus Nijhoff, The Hague, 1983) p. 589.

*Received 20 July 1992  
and accepted 16 April 1993*